Journal of Magnetic Resonance 306 (2019) 150–154

Contents lists available at ScienceDirect

Journal of Magnetic Resonance

journal homepage: www.elsevier.com/locate/jmr

Multiple dimensions for random walks

Daniel Topgaard

Physical Chemistry, Lund University, Lund, Sweden

ARTICLE INFO

Article history:
Received 24 March 2019
Revised 7 June 2019
Accepted 8 July 2019
Available online 9 July 2019

Keywords:
Magnetic resonance
Multidimensional
Diffusion
Flow
Restriction
Anisotropy
Exchange
Microstructure

ABSTRACT

Current trends in diffusion NMR and MRI methods development are reviewed. While great efforts are still directed towards further improving the spectral, spatial, and relaxation rate resolution of basic diffusion measurements, recent improvements in magnetic field gradient technology on whole-body scanners have enabled an exciting line of research involving MRI implementations of advanced diffusion NMR methods with motion-encoding gradient waveforms designed for multidimensional separation and correlation of properties like short-time diffusivity, restriction, anisotropy, flow, and exchange, thereby opening up for highly specific characterization of microstructure and heterogeneity in healthy and diseased tissues in a clinical setting.

1. Introduction

Diffusion NMR and MRI [1–3] are today used in the fields of chemistry, porous media, and neuroscience to investigate molecular and microstructural properties such as molecular weights [4], self-association in solution [5], compartment sizes [6], and surface-to-volume ratios [7]. Already in the 50 s it was noted that magnetic field gradients encode the NMR signal with information about self-diffusion [8] and flow [9], a decade later being followed by papers about restrictions [10], anisotropy [11], heterogeneity [12], and exchange [13]. Investigations of multi-component liquid solutions, materials, and biological tissues were enabled by combining the diffusion encoding with chemical shift resolution [14], imaging [15], and relaxometry [16]. Although diffusion NMR has a history of nearly 70 years, it remains a subject of intense research both in terms of basic methods development and new applications. While NMR of porous media should get the credit for most of the basic theory and methods development [1,2], clinical MRI has over the last decade become the largest and most important application area [3]. This special issue contribution gives the author's personal views on current trends in the field of diffusion NMR and MRI focusing on the recent translation of advanced diffusion encoding methods from the field of porous media into the context of clinical MRI.

2. Improving the spectral, spatial, and relaxation resolution

For isotropic solutions where all molecular-scale dynamics are orders of magnitude faster than the 1–1000 ms time scale of diffusion encoding, species-resolved self-diffusion coefficients represent the maximum amount of information that can be extracted. Consequently, diffusion NMR developments for chemistry applications focus on improving the resolution of chemical species by, e.g., suppressing the water signal [17] and *J*-coupling multiplets [18], as well as by including multiple spectral dimensions [19] – sometimes combined with non-uniform sampling to reduce the measurement time [20]. Correspondingly, within diffusion MRI great efforts are directed towards improving the spatial resolution [21] and reducing image artifacts [22]. When applying diffusion NMR to heterogeneous and porous materials like rocks, plants, and food products, species resolution based on the chemical shift is often prevented by line broadening caused by differences in magnetic susceptibility between the microscopic domains of the material. As a substitute for chemical shift resolution, differences in relaxation rates have proven to be efficient in resolving signals of the constituents [16]. Inclusion of multiple relaxation dimensions further improves the resolution [23] and spatial encoding of the indirect dimension leads to reductions in measurement time [24]. Additional improvements are obtained by introducing relaxation-diffusion correlation into a protocol with spatial resolution [25] and a combination of spatial selectivity and spectroscopic resolution [26].

E-mail address: daniel.topgaard@fkem1.lu.se

https://doi.org/10.1016/j.jmr.2019.07.024
1090-7807/

3. Heterogeneous materials and the curse of sensitivity

Even after all efforts of improving the spatial resolution, the voxels in clinical MRI have dimensions on the millimeter scale which is about two orders of magnitude larger than the micrometer-scale diffusional displacements during the motion-encoding gradients. Hence, the signal from each voxel may contain unresolved contributions from multiple environments with distinct diffusion properties. The translational motion of water in living biological tissues is affected by the microscopic barriers formed by macromolecules and partially permeable and orientationally ordered biomembranes, as well as by flow in the microcapillary network. Diffusion MRI is conventionally performed with the pulsed gradient spin echo (PGSE) experiment [27], which is excellent for measuring self-diffusion coefficients in liquids but is also sensitive to properties like flow [9], restrictions [10], anisotropy [11], heterogeneity [12], and exchange [13]. Contemporary diffusion MRI literature abounds with methods such as IVIM [28], DKI [29], HARDI [30], DSI [31], DBSI [32], NODDI [33], RSI [34], VERDICT [35], MSMT-CSD [36], CTRW [37], DIAMOND [38], and SMT [39], which claim to measure different properties but are all based on ambiguous PGSE data that, depending on one's preferences, may be attributed to any of the potentially contributing mechanisms. The sensitivity of the PGSE experiment to multiple molecular and microstructural properties is the very basis for its success in solving a wide range of scientific problems, but is also a nuisance when attempting to study complex materials like living biological tissues where it cannot be safely assumed which of the candidate properties that dominate the experimental observations.

4. Introducing specificity in motion encoding

Greater specificity can be achieved with gradient waveforms designed for removing or isolating the effects of some particular aspect of motion: notable examples include restrictions [40], anisotropy [41], flow [9], and exchange [42]. In the limit of high oscillation frequencies, the gradient waveform $G_i(t)$ in Fig. 1(a) gives signal attenuation originating solely from the short-time diffusivity independent of restrictions, anisotropy, and flow. The waveform comprises frequency- and amplitude-modulated oscillations which upon integration over time yields a dephasing vector $q_i(t)$ performing a trajectory inspired by the double rotation technique in solid-state NMR [43] and a dephasing spectrum $F_{ij}(t)$ [44] with nearly equal high-frequency peaks and identical zeroth moments along the diagonal $ij = xx$, yy, zz, resulting in isotropic diffusion weighting [41]. Insensitivity to flow corresponds to vanishing first moments of $G_i(t)$, time-averages of $q_i(t)$, and zero-frequency lobes of $F_{ij}(\omega)$. The reduced oscillation frequency in Fig. 1(b) introduces the effects of restricted diffusion [10] while remaining insensitive to anisotropy and flow. Limiting the gradients to a single axis in Fig. 1(c) brings in the effects of anisotropy [11], while the non-zero first moments of $G_i(t)$ in Fig. 1(d) gives sensitivity to flow [9]. The effects of relaxation [16] and exchange [42] are separated from motion-encoding by introducing time periods where $q(t) = 0$ as in Fig. 1(e) and (f). The Fig. 1(d) waveform corresponds to the PGSE experiment [27] which is the basis for conventional diffusion NMR and MRI and whose sensitivity to a plethora of motion properties has given rise to the profusion of methods in diffusion MRI [28–39].

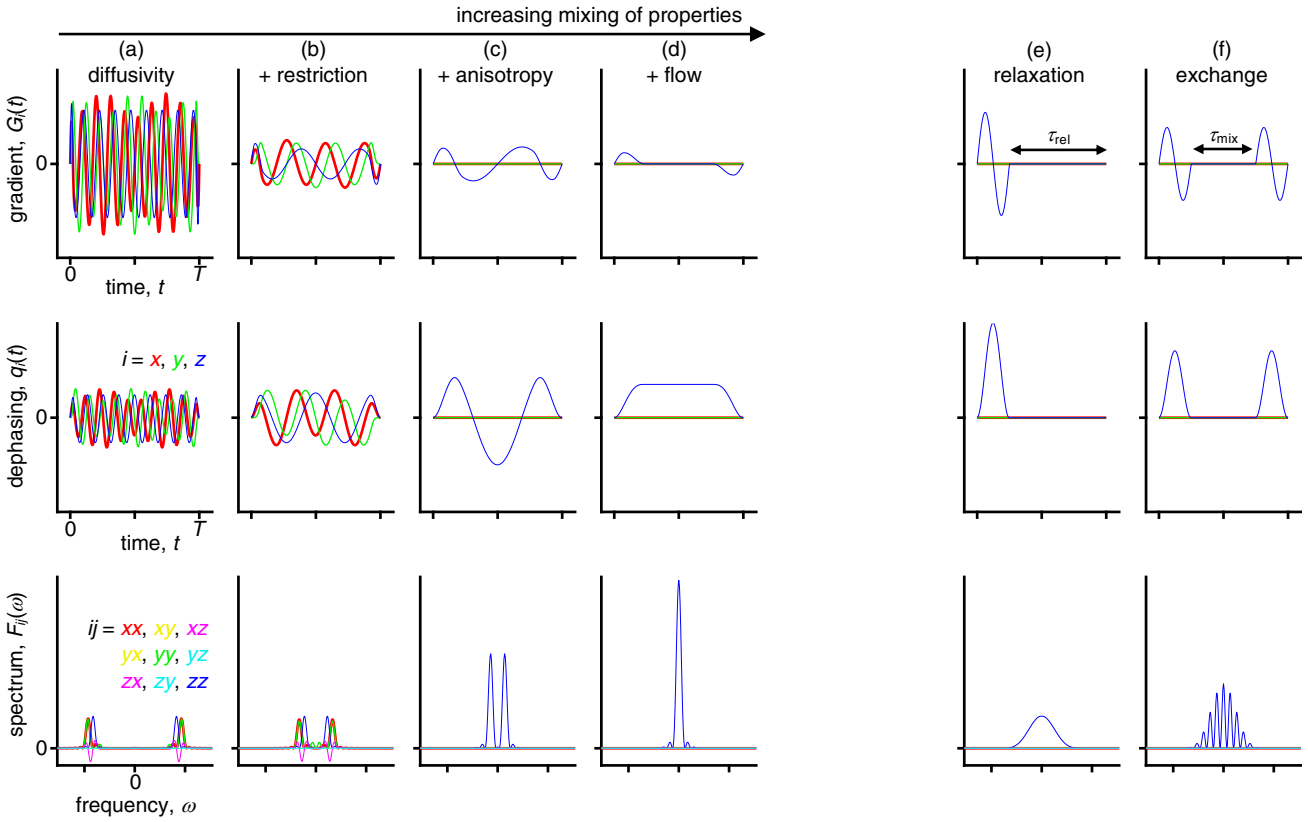

Fig. 1. Time-dependent magnetic field gradients $G_i(t)$ and dephasing vectors $q_i(t)$ with corresponding dephasing spectra $F_{ij}(\omega)$ targeting specific modes of translational motion. (a) Three-dimensional high-frequency modulation encoding for short-time diffusivity. (b) Low-frequency modulation introducing the effects of restrictions. (c) Low-dimensional modulation introducing the effects of anisotropy. (d) Non-zero first moment of $G_i(t)$ introducing sensitivity to flow. (e) Separation of motion-encoding gradients and time period τ_{rel} encoding for relaxation. (f) Separation of motion-encoding gradients into two blocks bracketing the time period τ_{mix} encoding for exchange. For all cases (a)–(f), the gradient amplitudes are scaled to give the same value of the diffusion-weighting variable b and the same signal attenuation for a homogeneous and isotropic liquid such as pure water under non-flowing conditions.

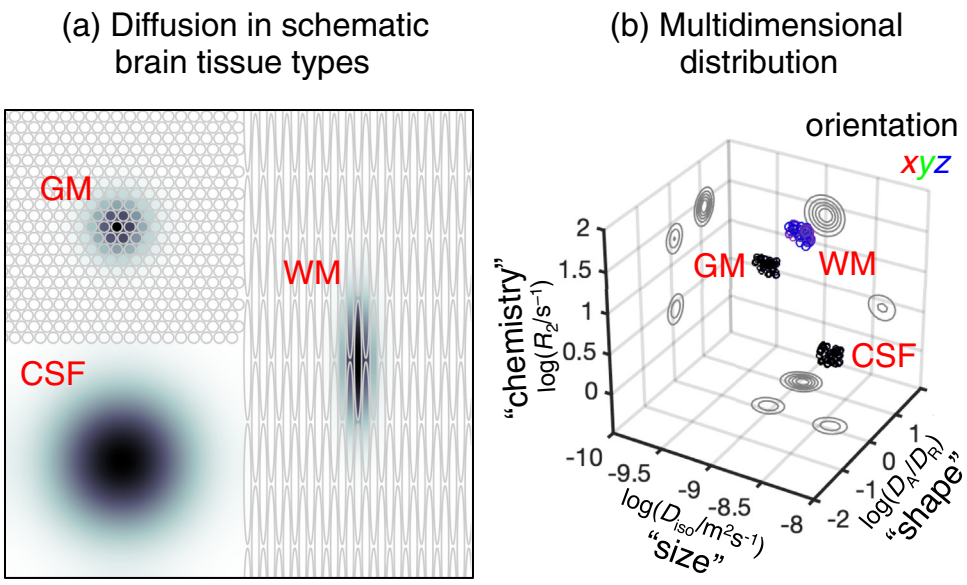

Fig. 2. Quantifying MRI voxel composition as a multidimensional distribution. (a) Schematic tissue microstructures with water diffusion patterns shown as "ink stains" with sizes, shapes, and orientations determined by the underlying cell structure. The highly simplified cartoons correspond to gray matter (GM), cerebrospinal fluid (CSF), and white matter (WM). Small diffusion patterns indicate small cells, high cell density, and/or low cell membrane permeability. (b) Multidimensional distribution where sub-voxel tissue regions are resolved by the sizes, shapes, and orientations of the water diffusion patterns, as well as by the local chemical composition of the water phase using the transverse relaxation rate R_2 as a proxy. The distribution is shown as a 3D scatter plot in a logarithmic space of R_2 ("chemistry"), isotropic diffusivity $D_{iso} = (D_A + 2D_R)/3$ ("size"), and axial-radial ratio D_A/D_R ("shape"), where D_A and D_R are the axial and radial diffusivities.

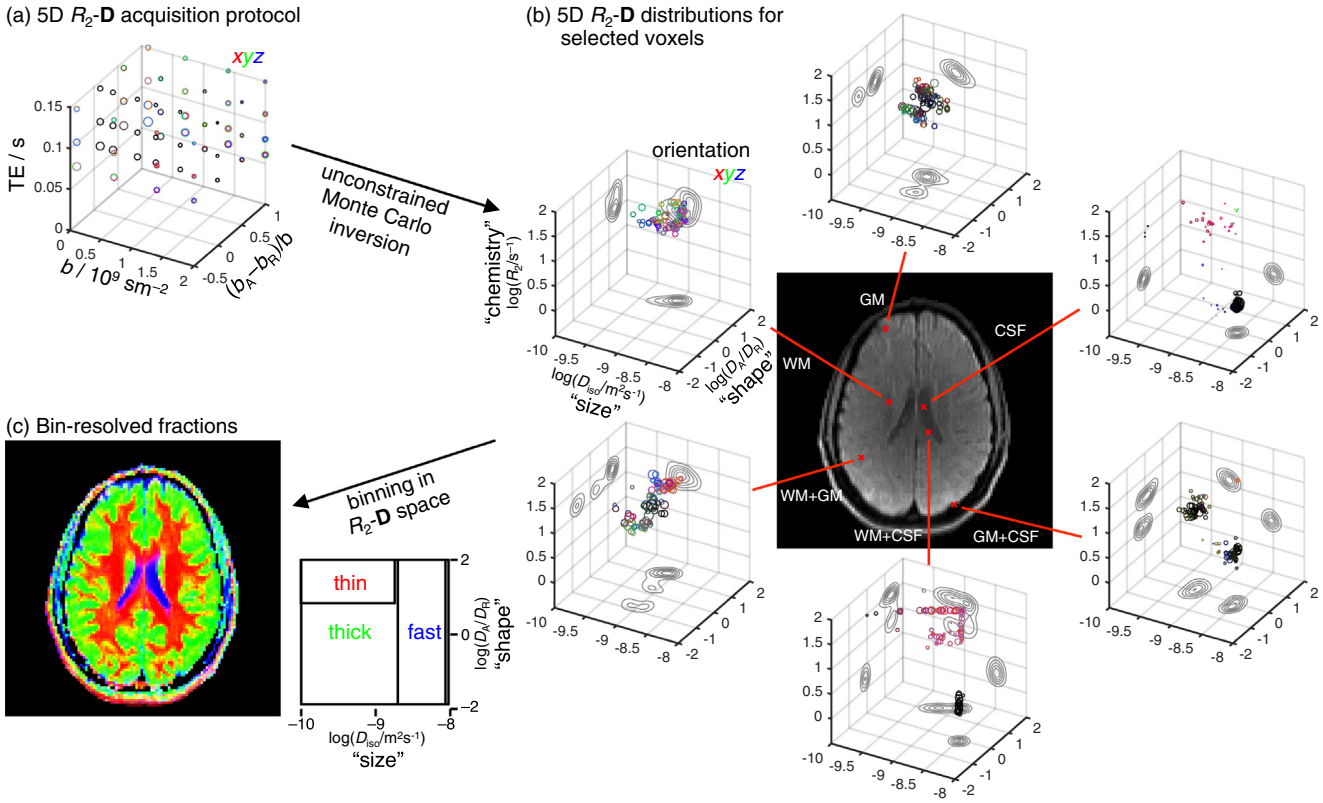

Fig. 3. In vivo 5D relaxation-diffusion (R_2-**D**) correlation MRI. (a) Signal acquired in a 5D space of axial and radial b-values, b_A and b_R, b-tensor orientation (Θ,Φ), and echo time (TE). The data is displayed as a 3D scatter plot with the axes b-tensor trace $b = b_A + 2b_R$, normalized b-tensor anisotropy $(b_A - b_R)/b$, and TE, using color-coding according to the Cartesian components of the orientation vector and circle area given by the signal intensity. (b) 5D relaxation-diffusion distributions with the dimensions axial and radial diffusivities, D_A and D_R, diffusion tensor orientation (θ,φ), and transverse relaxation rate R_2. The distributions are shown as 3D logarithmic plots of $D_{iso} = (D_A + 2D_R)/3$, D_A/D_R, and R_2, corresponding to the "size", "shape", and "chemistry" properties in Fig. 2(b). The selected voxels contain white matter (WM), gray matter (GM), and cerebrospinal fluid (CSF), as well as the binary combinations WM + GM, WM + CSF, and GM + CSF. (c) Color-coded composite image of the fractional populations in the "thin" (red), "thick" (green), and "fast" (blue) bins in the 2D "size"-"shape" projection of the 5D relaxation-diffusion space. Voxels containing more than one fraction are visible as mixed colors, e.g. thin + thick (yellow), thin + fast (purple), and thick + fast (turquoise). (Data from Martins et al. [67] and Tax et al. [68].) (For interpretation of the references to color in this figure legend, the reader is referred to the web version of this article.)

For a homogeneous and isotropic liquid where the details about translational motion are fully captured with self-diffusion coefficients, the gradient waveforms in Fig. 1 would all give the same signal attenuation. By comparing results obtained with different waveforms, mechanisms other than simple isotropic diffusion can be unambiguously proven, for instance restrictions [40], anisotropy [45], flow [9], and exchange [46]. The price for selectivity is paid in a currency of gradient amplitudes required to obtain a certain amount of diffusion weighting. The most selective waveform in Fig. 1(a) also requires the highest gradient amplitudes, which may be challenging to achieve on conventional clinical scanners. With the recent availability of high-amplitude and -precision gradients on whole-body scanners, most of the specific motion-encoding waveforms have now been applied in vivo not only for animals [47–50] but also for humans [41,51–60].

5. Multidimensional separation and correlation

Within the field of NMR of porous media, some of the Fig. 1 waveforms for probing specific aspects of translational motion have been incorporated into a multidimensional framework deriving from NMR spectroscopy [61–66]. This framework facilitates rational design of acquisition protocols and analysis approaches with commensurate levels of detail. As a general rule, each estimated property should be probed with a specific acquisition variable. An example of the multidimensional concept is given in Fig. 2 showing schematic tissue microstructures with diffusion propagators illustrated as "ink stains" with sizes and shapes determined by the interplay between the short-time diffusivity and the geometry and permeability of the cell membranes. The tissue components are resolved in the multidimensional "size"-"shape"-orien tation-"chemistry" distribution in Fig. 2(b) which can be estimated with an acquisition protocol encoding for the corresponding properties as shown in Fig. 3 [67,68].

6. Outlook

This summary of state-of-the-art in the field will hopefully encourage researchers following the mainstream trend of applying increasingly detailed constraints and prior knowledge (or wishful thinking) in an attempt to extract more details from conventional PGSE data [28–39], to instead develop multidimensional acquisition protocols and analysis approaches with appropriate balance between encoded and extracted information. In principle, it is possible to generalize the multidimensional correlation concept to all of the properties in Fig. 1, giving a "Mother of all correlations" protocol with acquisition variables encoding for correlations between short-time diffusivity, restriction, anisotropy, flow, relaxation, and exchange. Such an exhaustive protocol should be seen as an ambitious goal that may not be fully reached on account of practical limitations on the total measurement time. Instead, lower-dimensional protocols targeting specific combinations of properties, like the one in Fig. 3, could be a reasonable compromise between scanner time and amount of obtained information.

Acknowledgments

This work was financially supported by the Swedish Foundation for Strategic Research (AM13-0090, ITM17-0267) and the Swedish Research Council (2018-03697). DT owns shares in Random Walk Imaging AB (Lund, Sweden, http://www.rwi.se/), holding patents related to the described methods.

References

[1] W.S. Price, NMR Studies of Translational Motion, Cambridge University Press, Cambridge, 2009.
[2] P.T. Callaghan, Translational Dynamics & Magnetic Resonance, Oxford University Press, Oxford, 2011.
[3] D.K. Jones, Diffusion MRI: Theory, Methods, and Applications, Oxford University Press, 2010.
[4] P.T. Callaghan, D.N. Pinder, A pulsed field gradient NMR study of self-diffusion in a polydisperse polymer system: dextran in water, Macromolecules 16 (1983) 968–973.
[5] P. Stilbs, B. Lindman, Determination of organic counterion binding to micelles through Fourier transform NMR self-diffusion measurements, J. Phys. Chem. 85 (1981) 2587–2589.
[6] K.J. Packer, C. Rees, Pulsed NMR studies of restricted diffusion. I. Droplet size distributions in emulsions, J. Colloid Interface Sci. 40 (1972) 206–218.
[7] L.L. Latour, P.P. Mitra, R.L. Kleinberg, C.H. Sotak, Time-dependent diffusion coefficient of fluids in porous media as a probe of surface-to-volume ratio, J. Magn. Reson. A 101 (1993) 342–346.
[8] E.L. Hahn, Spin echoes, Phys. Rev. 80 (1950) 580–594.
[9] H.Y. Carr, E.M. Purcell, Effects of diffusion on free precession in nuclear magnetic resonance experiments, Phys. Rev. 94 (1954) 630–638.
[10] D.E. Woessner, N.M.R. spin-echo self-diffusion measurements on fluids undergoing restricted diffusion, J. Phys. Chem. 67 (1963) 1365–1367.
[11] B.D. Boss, E.O. Stejskal, Anisotropic diffusion in hydrated vermiculite, J. Chem. Phys. 43 (1965) 1068–1069.
[12] B.D. Boss, E.O. Stejskal, J.D. Ferry, Self-diffusion in high molecular weight polyisobutylene-benzene mixtures determined by the pulsed-gradient, spin-echo method, J. Phys. Chem. 71 (1967) 1501–1506.
[13] J. Kärger, Zur Bestimmung der Diffusion in einem Zweibereichsystem mit Hilfe von gepulsten Feldgradienten, Ann. Phys. 479 (1969) 1–4.
[14] T.L. James, G.G. McDonald, Measurement of the self-diffusion coefficient of each component in a complex system using pulsed-gradient Fourier transform NMR, J. Magn. Reson. 11 (1973) 58–61.
[15] K.-D. Merboldt, W. Hänicke, J. Frahm, Self-diffusion NMR imaging using stimulated echoes, J. Magn. Reson. 64 (1985) 479–486.
[16] D. van Dusschoten, P.A. de Jager, H. Van As, Extracting diffusion constants from echo-time-dependent PFG NMR data using relaxation-time information, J. Magn. Reson. A 116 (1995) 22–28.
[17] G. Zheng, T. Stait-Gardner, P.G.A. Kumar, A.M. Torres, W.S. Price, PGSTE-WATERGATE: an STE-based PGSE NMR sequence with excellent solvent suppression, J. Magn. Reson. 191 (2008) 159–163.
[18] M. Foroozandeh, L. Castanar, L.G. Martins, D. Sinnaeve, G.D. Poggetto, C.F. Tormena, R.W. Adams, G.A. Morris, M. Nilsson, Ultrahigh-resolution diffusion-ordered spectroscopy, Angew. Chem. Int. Ed. Engl. 55 (2016) 15579–15582.
[19] E.K. Gozansky, D.G. Gorenstein, DOSY-NOESY: diffusion-ordered NOESY, J. Magn. Reson. B 111 (1996) 94–96.
[20] G.N. Manjunatha Reddy, M. Yemloul, S. Caldarelli, Combined maximum-quantum and DOSY 3D experiments provide enhanced resolution for small molecules in mixtures, Magn. Reson. Chem. 55 (2017) 492–497.
[21] S.J. Holdsworth, R. O'Halloran, K. Setsompop, The quest for high spatial resolution diffusion-weighted imaging of the human brain in vivo, NMR Biomed. 32 (2019) e4056.
[22] E. Solomon, G. Liberman, N. Nissan, L. Frydman, Robust diffusion tensor imaging by spatiotemporal encoding: principles and in vivo demonstrations, Magn. Reson. Med. 77 (2017) 1124–1133.
[23] B. Sun, K.-J. Dunn, A global inversion method for multi-dimensional NMR logging, J. Magn. Reson. 172 (2005) 152–160.
[24] S. Ahola, V.V. Zhivonitko, O. Mankinen, G. Zhang, A.M. Kantola, H.Y. Chen, C. Hilty, I.V. Koptyug, V.V. Telkki, Ultrafast multidimensional Laplace NMR for a rapid and sensitive chemical analysis, Nat. Commun. 6 (2015) 8363.
[25] Y. Zhang, B. Blümich, Spatially resolved D-T2 correlation NMR of porous media, J. Magn. Reson. 242 (2014) 41–48.
[26] N. Shemesh, J.T. Rosenberg, J.N. Dumez, J.A. Muniz, S.C. Grant, L. Frydman, Metabolic properties in stroked rats revealed by relaxation-enhanced magnetic resonance spectroscopy at ultrahigh fields, Nat. Commun. 5 (2014) 4958.
[27] E.O. Stejskal, J.E. Tanner, Spin diffusion measurements: spin echoes in the presence of a time-dependent field gradient, J. Chem. Phys. 42 (1965) 288–292.
[28] D. Le Bihan, R. Turner, C.T.W. Moonen, J. Pekar, Imaging of diffusion and microcirculation with gradient sensitization: design, strategy, and significance, J. Magn. Reson. Imag. 1 (1991) 7–28.
[29] J.H. Jensen, J.A. Helpern, A. Ramani, H. Lu, K. Kaczynski, Diffusional kurtosis imaging: the quantification of non-Gaussian water diffusion by means of magnetic resonance imaging, Magn. Reson. Med. 53 (2005) 1432–1440.
[30] D.S. Tuch, T.G. Reese, M.R. Wiegell, N. Makris, J.W. Belliveau, V.J. Wedeen, High angular resolution diffusion imaging reveals intravoxel white matter fiber heterogeneity, Magn. Reson. Med. 48 (2002) 577–582.
[31] V.J. Wedeen, P. Hagmann, W.Y. Tseng, T.G. Reese, R.M. Weisskoff, Mapping complex tissue architecture with diffusion spectrum magnetic resonance imaging, Magn. Reson. Med. 54 (2005) 1377–1386.
[32] Y. Wang, Q. Wang, J.P. Haldar, F.C. Yeh, M. Xie, P. Sun, T.W. Tu, K. Trinkaus, R.S. Klein, A.H. Cross, S.K. Song, Quantification of increased cellularity during inflammatory demyelination, Brain 134 (2011) 3590–3601.

[33] H. Zhang, T. Schneider, C.A. Wheeler-Kingshott, D.C. Alexander, NODDI: Practical in vivo neurite orientation dispersion and density imaging of the human brain, Neuroimage 61 (2012) 1000–1016.
[34] N.S. White, T.B. Leergaard, H. D'Arceuil, J.G. Bjaalie, A.M. Dale, Probing tissue microstructure with restriction spectrum imaging: Histological and theoretical validation, Hum. Brain Mapp. 34 (2013) 327–346.
[35] E. Panagiotaki, S. Walker-Samuel, B. Siow, S.P. Johnson, V. Rajkumar, R.B. Pedley, M.F. Lythgoe, D.C. Alexander, Noninvasive quantification of solid tumor microstructure using VERDICT MRI, Cancer Res. 74 (2014) 1902–1912.
[36] B. Jeurissen, J.-D. Tournier, T. Dhollander, A. Connelly, J. Sijbers, Multi-tissue constrained spherical deconvolution for improved analysis of multi-shell diffusion MRI data, Neuroimage 103 (2014) 411–426.
[37] M.M. Karaman, Y. Sui, H. Wang, R.L. Magin, Y. Li, X.J. Zhou, Differentiating low- and high-grade pediatric brain tumors using a continuous-time random-walk diffusion model at high b-values, Magn. Reson. Med. 76 (2016) 1149–1157.
[38] B. Scherrer, A. Schwartzman, M. Taquet, M. Sahin, S.P. Prabhu, S.K. Warfield, Characterizing brain tissue by assessment of the distribution of anisotropic microstructural environments in diffusion-compartment imaging (DIAMOND), Magn. Reson. Med. 76 (2016) 963–977.
[39] E. Kaden, F. Kruggel, D.C. Alexander, Quantitative mapping of the per-axon diffusion coefficients in brain white matter, Magn. Reson. Med. 75 (2016) 1752–1763.
[40] J.E. Tanner, Self diffusion of water in frog muscle, Biophys. J. 28 (1979) 107–116.
[41] S. Mori, P.C.M. van Zijl, Diffusion weighting by the trace of the diffusion tensor within a single scan, Magn. Reson. Med. 33 (1995) 41–52.
[42] D.G. Cory, A.N. Garroway, J.B. Miller, Applications of spin transport as a probe of local geometry, Polym. Prepr. 31 (1990) 149–150.
[43] A. Samoson, E. Lippmaa, A. Pines, High resolution solid-state NMR: averaging of second-order effects by means of a double-rotor, Mol. Phys. 65 (1998) 1013–1018.
[44] P.T. Callaghan, J. Stepisnik, Frequency-domain analysis of spin motion using modulated-gradient NMR, J. Magn. Reson. A 117 (1995) 118–122.
[45] S. Eriksson, S. Lasič, D. Topgaard, Isotropic diffusion weighting by magic-angle spinning of the *q*-vector in PGSE NMR, J. Magn. Reson. 226 (2013) 13–18.
[46] T.X. Cai, D. Benjamini, M.E. Komlosh, P.J. Basser, N.H. Williamson, Rapid detection of the presence of diffusion exchange, J. Magn. Reson. 297 (2018) 17–22.
[47] M.D. Does, E.C. Parsons, J.C. Gore, Oscillating gradient measurements of water diffusion in normal and globally ischemic rat brain, Magn. Reson. Med. 49 (2003) 206–215.
[48] B.A. Moffat, D.E. Hall, J. Stojanovska, P.J. McConville, J.B. Moody, T.L. Chenevert, A. Rehemtulla, B.D. Ross, Diffusion imaging for evaluation of tumor therapies in preclinical animal models, MAGMA 17 (2004) 249–259.
[49] F. Schilling, S. Ros, D.-E. Hu, P. D'Santos, S. McGuire, R. Mair, A.J. Wright, E. Mannion, R.J.M. Franklin, A.A. Neves, K.M. Brindle, MRI measurements of reporter-mediated increases in transmembrane water exchange enable detection of a gene reporter, Nat. Biotech. 35 (2017) 75–80.
[50] A. Ianus, N. Shemesh, Incomplete initial nutation diffusion imaging: an ultrafast, single-scan approach for diffusion mapping, Magn. Reson. Med. 79 (2018) 2198–2204.
[51] C.B. Ahn, S.Y. Lee, O. Nalcioglu, Z.H. Cho, The effects of random directional distributed flow in nuclear magnetic resonance imaging, Med. Phys. 14 (1987) 43–48.
[52] M. Nilsson, J. Lätt, D. van Westen, S. Brockstedt, S. Lasič, F. Ståhlberg, D. Topgaard, Noninvasive mapping of water diffusional exchange in the human brain using filter-exchange imaging, Magn. Reson. Med. 69 (2013) 1573–1581.
[53] C.A. Baron, C. Beaulieu, Oscillating gradient spin-echo (OGSE) diffusion tensor imaging of the human brain, Magn. Reson. Med. 72 (2014) 726–736.
[54] F. Szczepankiewicz, S. Lasič, D. van Westen, P.C. Sundgren, E. Englund, C.-F. Westin, F. Ståhlberg, J. Lätt, D. Topgaard, M. Nilsson, Quantification of microscopic diffusion anisotropy disentangles effects of orientation dispersion from microstructure: applications in healthy volunteers and in brain tumors, Neuroimage 104 (2015) 241–252.
[55] A. Wetscherek, B. Stieltjes, F.B. Laun, Flow-compensated intravoxel incoherent motion diffusion imaging, Magn. Reson. Med. 74 (2015) 410–419.
[56] A. Ahlgren, L. Knutsson, R. Wirestam, M. Nilsson, F. Ståhlberg, D. Topgaard, S. Lasič, Quantification of microcirculatory parameters by joint analysis of flow-compensated and non-flow-compensated intravoxel incoherent motion (IVIM) data, NMR Biomed. 29 (2016) 640–649.
[57] S. Vellmer, R. Stirnberg, D. Edelhoff, D. Suter, T. Stöcker, I.I. Maximov, Comparative analysis of isotropic diffusion weighted imaging sequences, J. Magn. Reson. 275 (2017) 137–147.
[58] G. Yang, J.A. McNab, Eddy current nulled constrained optimization of isotropic diffusion encoding gradient waveforms, Magn. Reson. Med. 81 (2019) 1818–1832.
[59] A.V. Avram, J.E. Sarlls, P.J. Basser, Measuring non-parametric distributions of intravoxel mean diffusivities using a clinical MRI scanner, Neuroimage 185 (2019) 255–262.
[60] K. Moulin, E. Aliotta, D.B. Ennis, Effect of flow-encoding strength on intravoxel incoherent motion in the liver, Magn. Reson. Med. 81 (2019) 1521–1533.
[61] P.T. Callaghan, B. Manz, Velocity exchange spectrosocpy, J. Magn. Reson. A 106 (1994) 260–265.
[62] R.G. Graham, W.C. Holmes, C. De Panfilis, K.J. Packer, Characterisation of locally anisotropic structures within isotropic porous solids using 2-D pulsed field gradient NMR, Chem. Phys. Lett. 332 (2000) 319–323.
[63] S.I. Han, S. Stapf, B. Blümich, Two-dimensional PFG NMR for encoding correlations of position, velocity, and acceleration in fluid transport, J. Magn. Reson. 146 (2000) 169–180.
[64] P.T. Callaghan, I. Furó, Diffusion-diffusion correlation and exchange as a signature for local order and dynamics, J. Chem. Phys. 120 (2004) 4032–4038.
[65] J.P. de Almeida Martins, D. Topgaard, Two-dimensional correlation of isotropic and directional diffusion using NMR, Phys. Rev. Lett. 116 (2016) 087601.
[66] D. Topgaard, Multidimensional diffusion MRI, J. Magn. Reson. 275 (2017) 98–113.
[67] J.P. de Almeida Martins, C. Tax, F. Szczepankiewicz, G. Eklund, K. Bryskhe, D.K. Jones, C.-F. Westin, D. Topgaard, Characterizing the microscopic heterogeneity of the living human brain with spatially resolved 5D diffusion-relaxation distributions, in: Experimental NMR Conference, Orlando, 2018, Poster 188.
[68] C.M.W. Tax, J.P. de Almeida Martins, F. Szczepankiewicz, C.-F. Westin, M. Chamberland, D. Topgaard, D.K. Jones, From physical chemistry to human brain biology: unconstrained inversion of 5-dimensional diffusion-T2 correlation data, Proc. Intl. Soc. Mag. Reson. Med. 26 (2018) 1101.